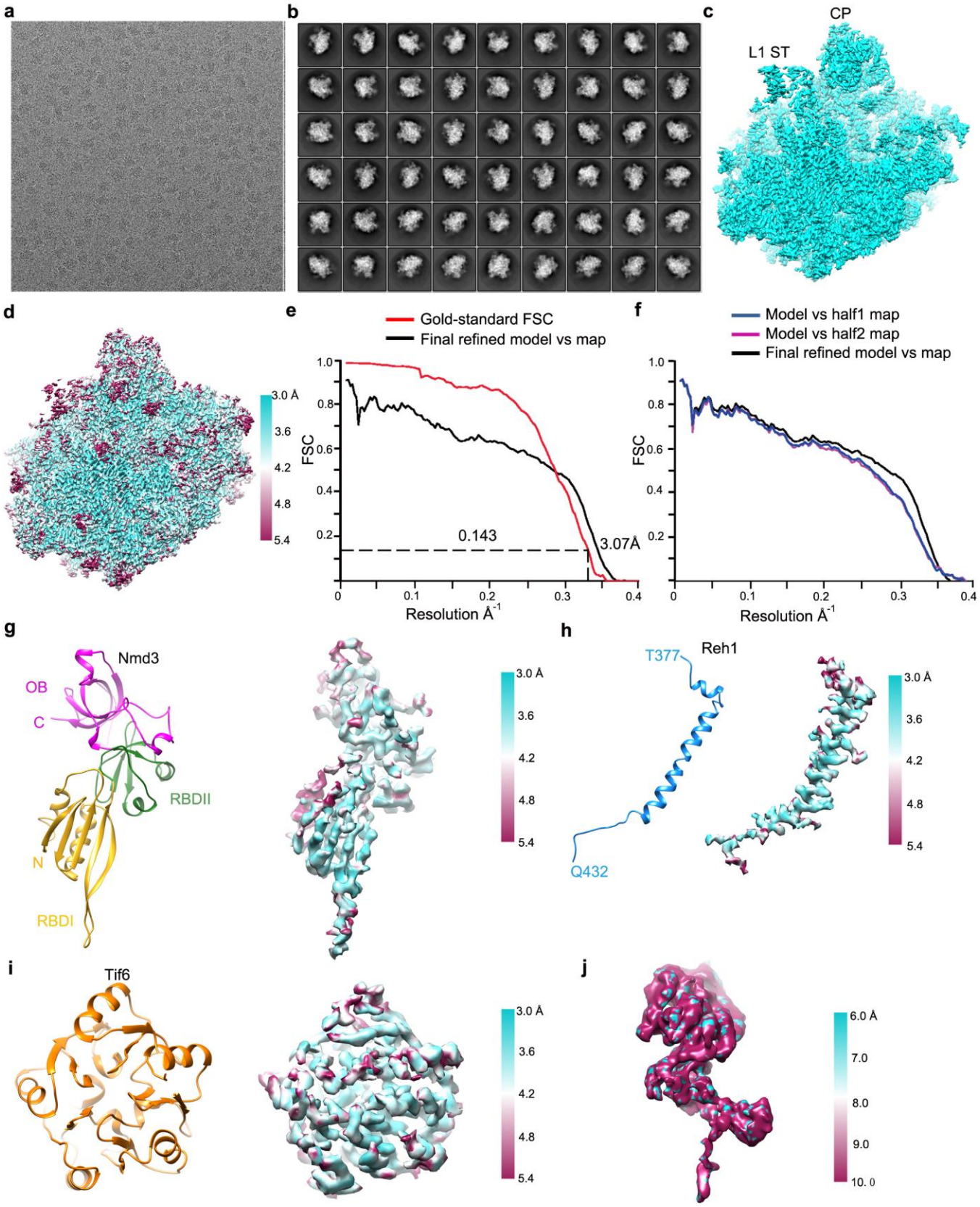

Supplementary Figure 1

Structural determination and model validation of the Nmd3-TAP pre-60S structure.

(**a**) A representative raw micrograph of the cryo-EM images. (**b**) Representative 2D class averages of cryo-EM particles. (**c**) The final density map of the Nmd3-TAP pre-60S particle in surface representation. (**d**) Local resolution map of the final density map. (**e**) Fourier shell correlation (FSC) curves for the final map after post-processing with RELION (red, gold-standard FSC), and for the cross-validation between final atomic model and the 3D density map (black, final refined model versus map). The overall resolution for the map is 3.07 Å. (**f**) The cross-validation FSC curves for the atomic model (blue, model versus half1 map, magenta, model versus half2 map, black, final refined model versus map). (**g**) The atomic model (left) and the local resolution map (right) of Nmd3, displayed in the same orientation. Note that one helix from RBDI is not resolved in side-chain resolution. (**h**) The atomic model (left) and the local resolution map (right) of Reh1, displayed in the same orientation. (**i**) The atomic model (left) and the local resolution map (right) of Tif6, displayed in the same orientation. (**j**) The local resolution map of Lsg1.

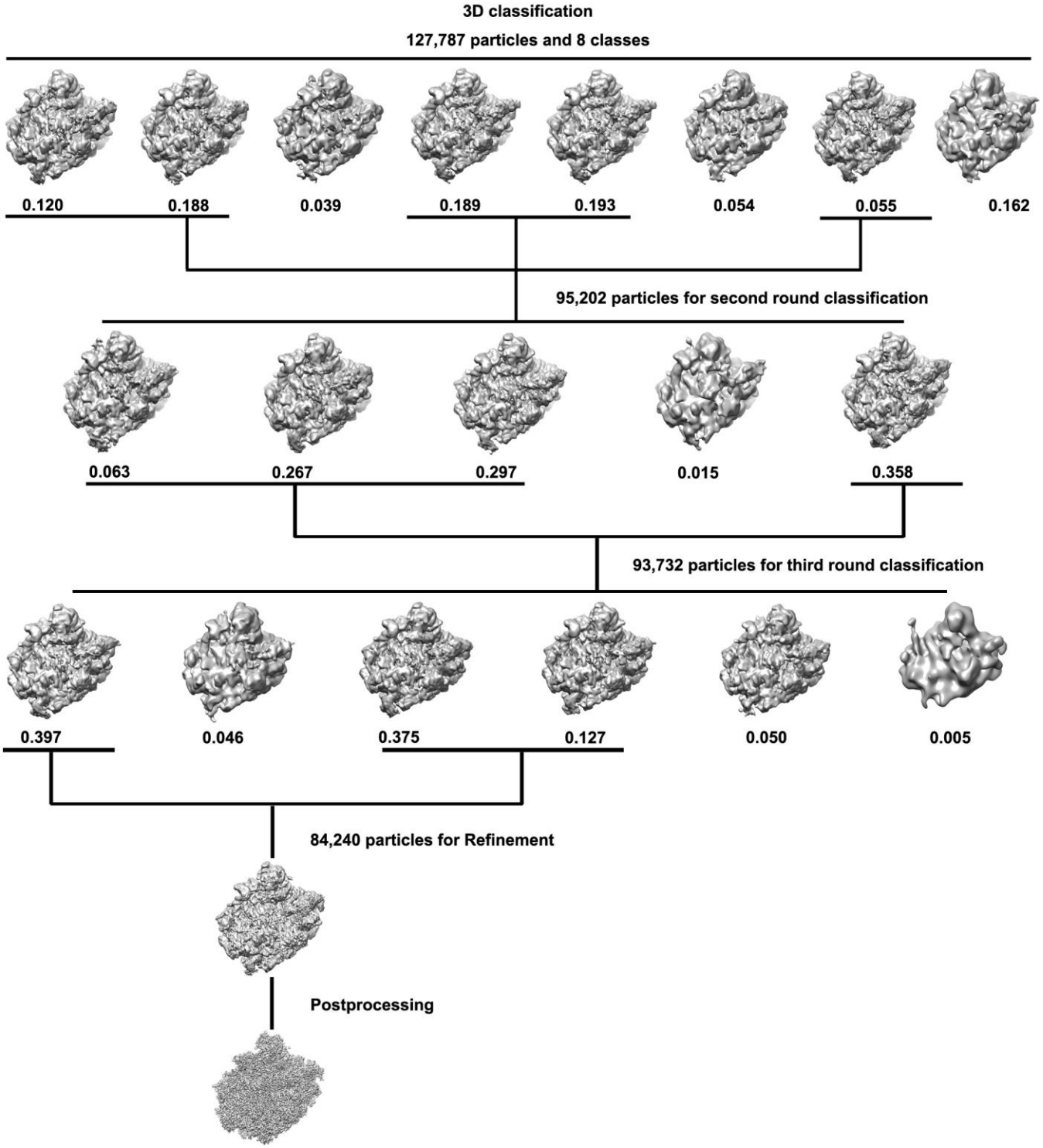

Supplementary Figure 2

The workflow of 3D classification.

Three rounds of 3D classification were performed and a final dataset of ~84k particles were used for refinement.

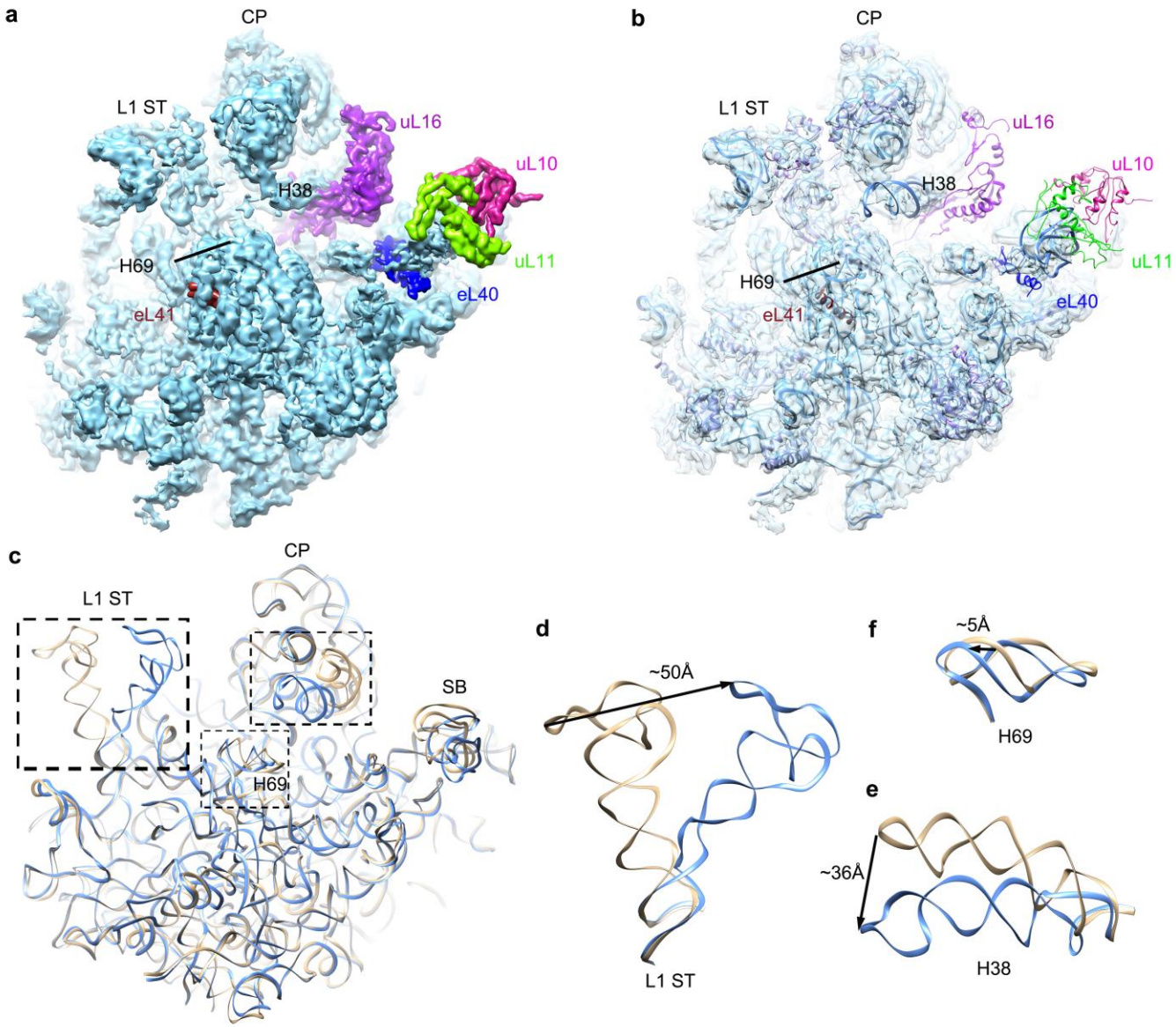

Supplementary Figure 3

Compositional and structural differences between the Nmd3 particle and the mature 60S subunit.

(**a**) Surface representation of the cryo-EM map of the Nmd3-particle. Ribosome proteins that are absent in the map are superimposed and separately colored. L1 ST, the L1 stalk; CP, central protuberance; SB, the P0 stalk base; H69, helix 69; H38, helix 38. (**b**) Same as **a**, but the map is shown in transparent surface representation, with atomic models superimposed. (**c**) Conformational differences of 25S rRNA in the mature 60S subunit (tan) and in the Nmd3-particle (blue). Coordinates of the mature 25S rRNA are from a crystal structure of the yeast 80S ribosome (PDB code 3U5E; Ben-Shem, A. *et al.*, Science **334**, 1524-1529, 2011). (**d-f**) Same as **c**, but in zoom-in views for three regions, L1 stalk (**d**), H38 (**e**) and H69 (**f**).

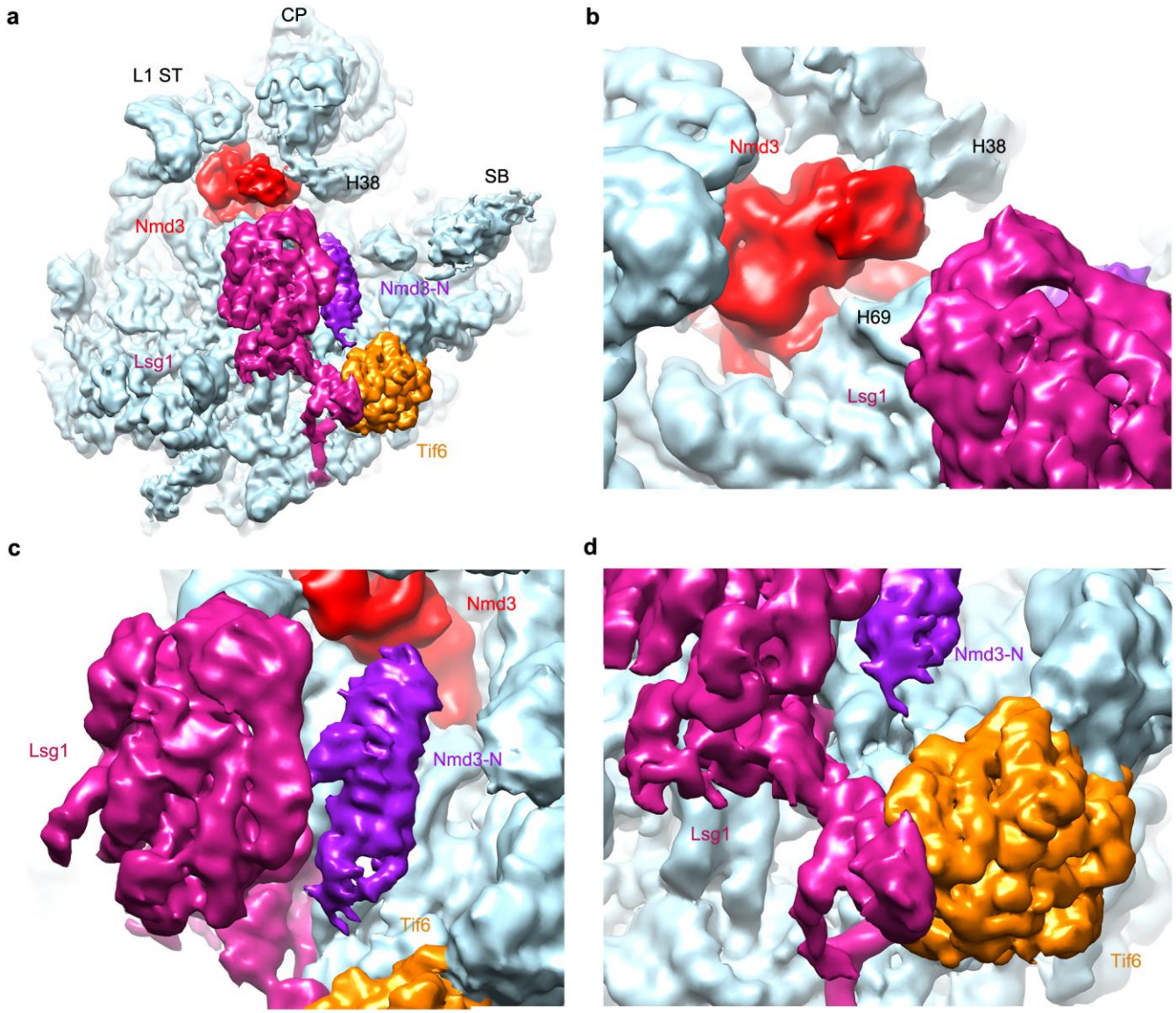

Supplementary Figure 4

Interactions of Lsg1 with Nmd3 and Tif6.

(**a**) The unsharpened cryo-EM map from “signal subtraction” method is shown in surface representation, with densities of factors colored separately. (**b**-**d**) Same as **a**, but in different zoom-in views, highlighting the interactions of Lsg1 with H69 (**b**), the N-terminal domain of Nmd3 (**c**), and Tif6 (**d**).

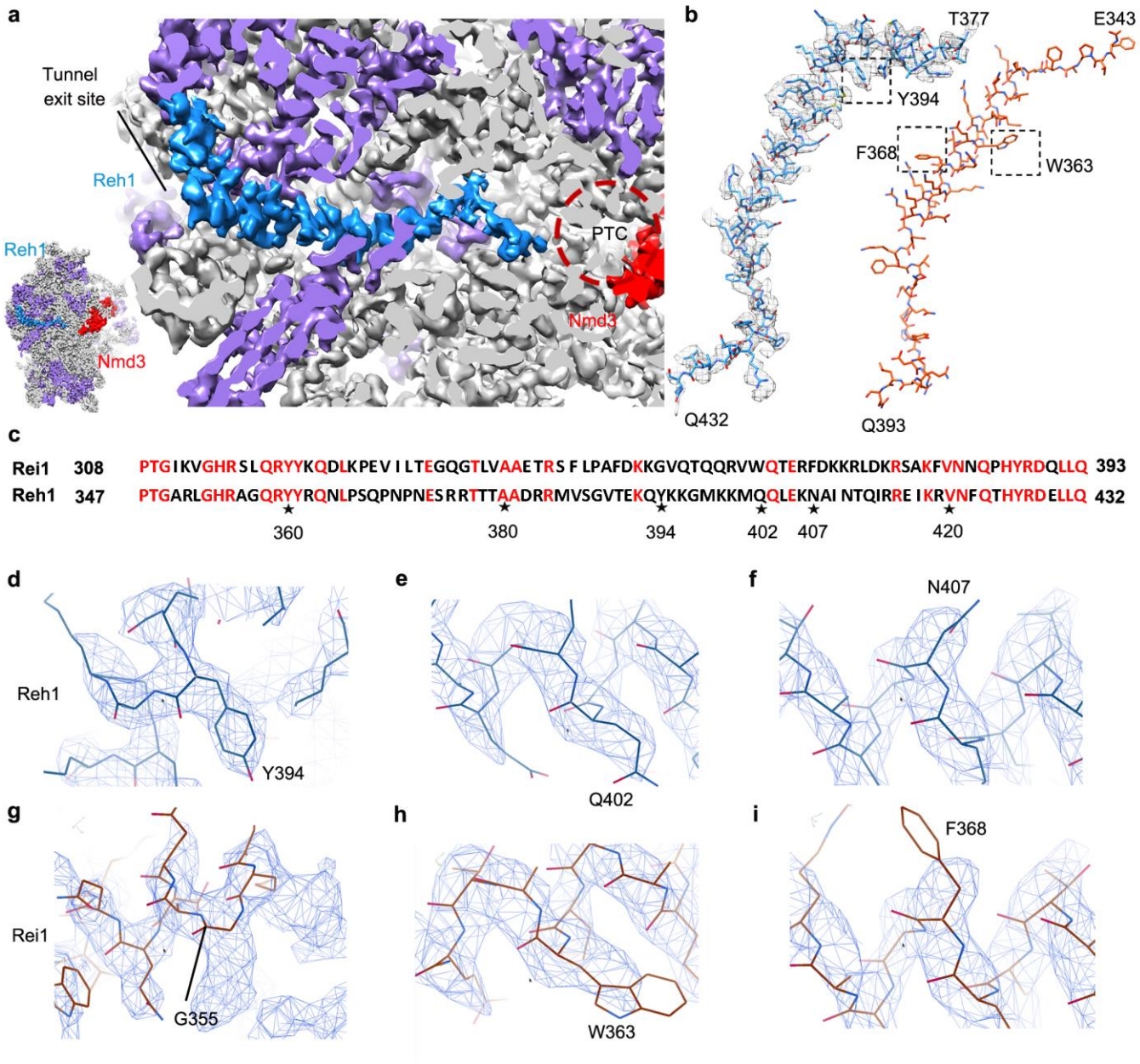

Supplementary Figure 5

Identification of the C terminus of Reh1 in the polypeptide exit tunnel.

(**a**) The sectional view of the cryo-EM map of the Nmd3-particle, highlighting the density in the tunnel (dodger blue). The PTC is marked with a dashed red circle. (**b**) The segmented density of the C-terminus of Reh1 is superimposed with the atomic model (left panel). The atomic model of the C-terminus of Rei1 (residues 343-393) is shown in the same orientation (right panel). (**c**) Sequence alignment of Reh1 and Rei1. (**d**-**f**) Line models of the sidechains of selected residues of Reh1, including Y394 (**d**), Q402 (**e**) and N407 (**f**), superimposed with the density map. (**g**-**i**) Line models of selected residues of Rei1, including G355 (**g**), W363 (**h**) and F368 (**i**), superimposed with the density map of the Nmd3-particle. Coordinates of Rei1 are from a previous study (PDB code 5APN; Greber, B.J. *et al.*, Cell **164**, 91-102, 2016).

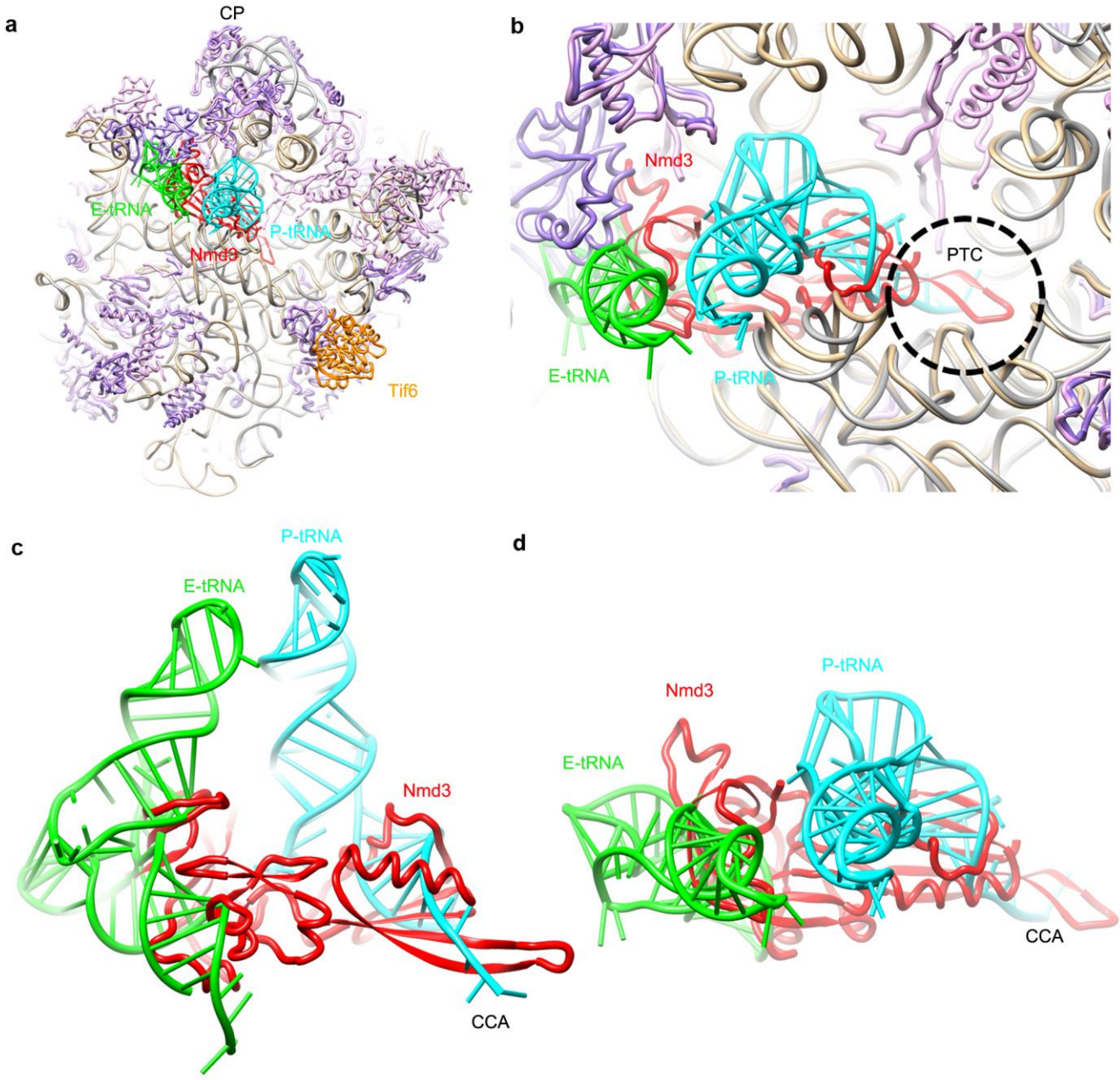

Supplementary Figure 6

Comparison of tRNAs with Nmd3 on the pre-60S structure.

(**a**) The atomic model of the Nmd3-particle, superimposed with aligned E-site and P-site tRNAs. Coordinates of tRNAs are from a previous work (PDB code 3J78; Svidritskiy, E. *et al.*, Structure **22**, 1210-1218, 2014). (**b**) Zoom-in view of **a**, highlighting the overlap between Nmd3 and the two tRNAs. The peptidyl transferase center (PTC) is marked by a dashed circle. (**c**-**d**) Same as **b**, but only tRNAs and Nmd3 are displayed. The CCA-end of the P-site tRNA is labelled.

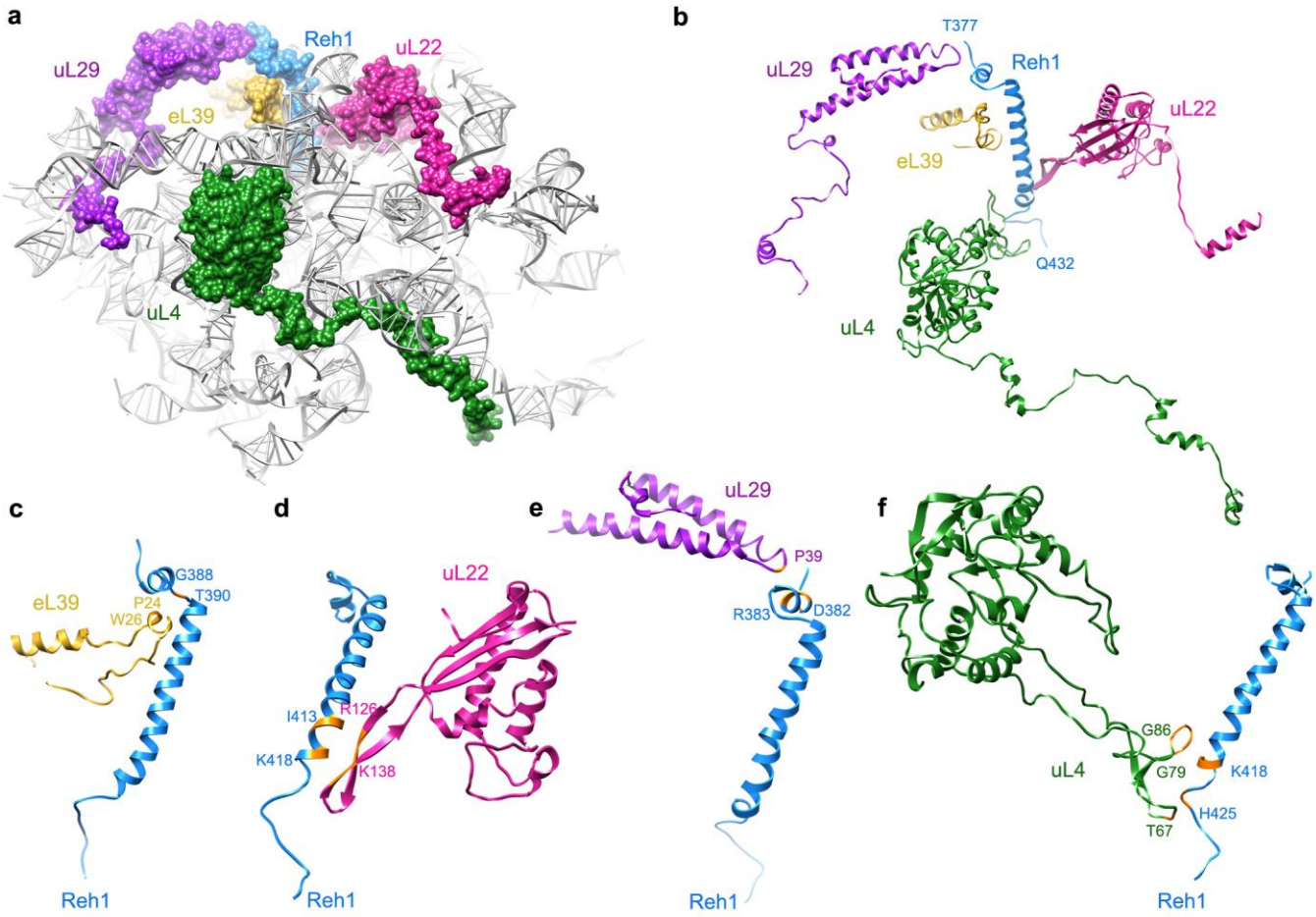

Supplementary Figure 7

Interactions of Reh1 with ribosomal proteins in the pre-60S particle.

(**a**-**f**) The interactions between Reh1 (dodger blue) and ribosomal proteins uL22, uL4, uL29, and eL39 (violet red, dark green, purple and gold, respectively). Sites of interactions are highlighted in bright orange.

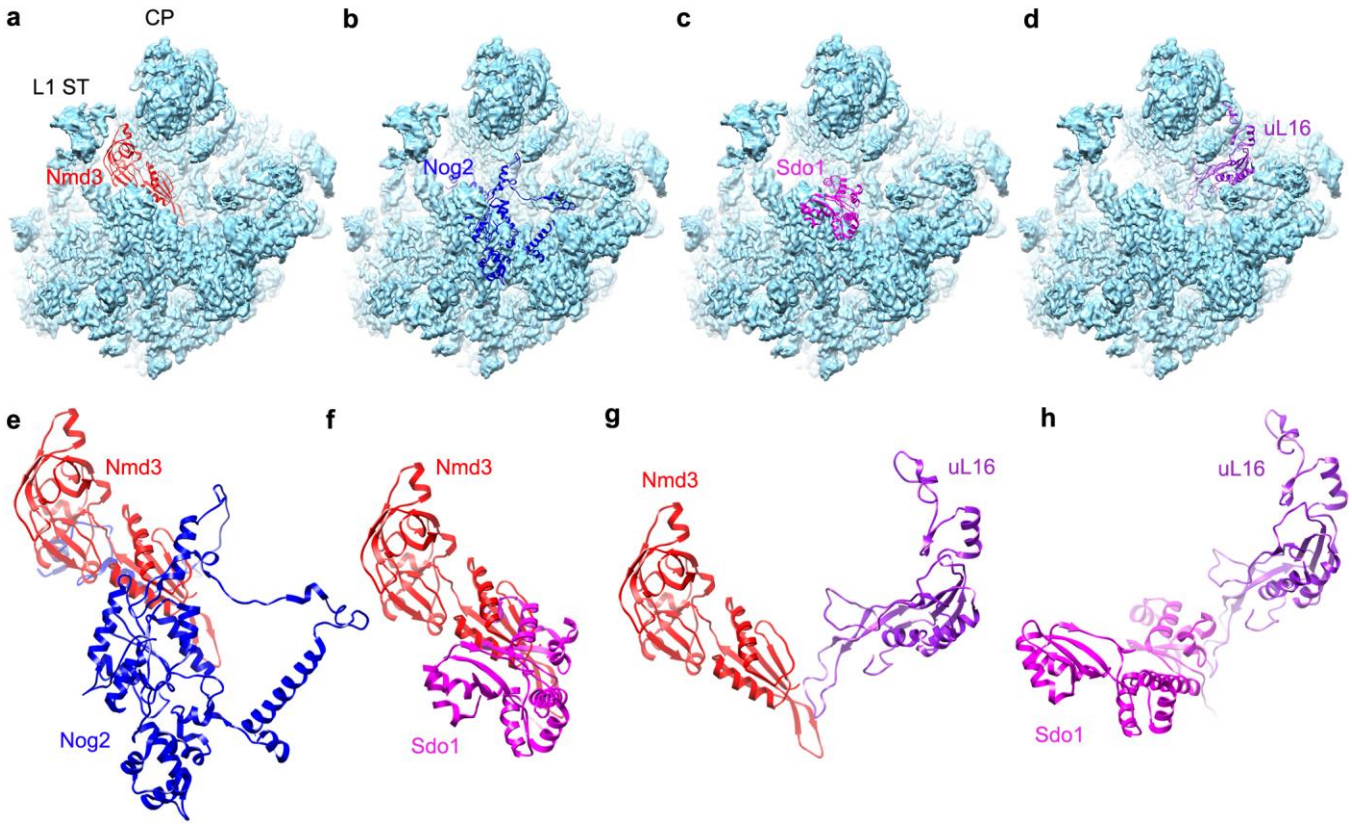

Supplementary Figure 8

Comparison of the binding sites of different assembly factors on the pre-60S particle.

(**a**-**d**) Atomic models of Nmd3, Nog2 (PDB code 3JCT; Wu, S. *et al.*, Nature **534**, 133-137, 2016), Sdo1 (PDB code 5ANB; *Weis, F. et al.*, Nature structural & molecular biology **22**, 914-919, 2015) and uL16 (PDB code 5ANB) are superimposed with the cryo-EM density map of the Nmd3-particle. (**e**) Structural conflict of Nmd3 and Nog2 on the pre-60S particle. (**f**) Structural conflict of Nmd3 and Sdo1 on the pre-60S particle. (**g**-**h**) Superimposition of uL16 with Nmd3 (**g**) and Sdo1 (**h**) on the pre-60S particle.

Supplementary Table 1. Mass spectrometry analysis of pre-60S particles.

Protein	MW [kDa]	Score	Coverage %
Ssa1	69.6	1894.43	73.52
Ssa2	69.4	1685.95	70.27
Lsg1	72.7	1143.53	70.47
Nmd3	59.1	1072.72	49.42
Reh1	49.7	618.48	45.14
Ssa4	69.6	536.88	35.51
Ssc1	70.6	502.07	53.82
Ssb2	66.6	478.12	50.57
Ssb1	66.6	473.92	53.18
Tif6	26.4	436.43	75.51
Arx1	65.2	337.75	44.69
Yvh1	41.2	331.61	62.09
Rpp0	33.7	331.38	39.10
Met17	48.6	229.94	39.19
Rei1	45.8	171.17	46.06